SINGLE RING MULTIBUNCH OPERATION AND BEAM SEPARATION

Richard Talman
Laboratory of Elementary-Particle Physics,
Cornell University

Abstract

The counter-circulating electrons and positrons in a circular Higgs Factory have to be separated everywhere except at the N^* intersection points (IP). The separation has to be electric and, to avoid unwanted increase of vertical emittance ϵ_y, the separation has to be horizontal. This paper considers only head-on collisions at $N^* = 2$ IP's, with the beams separated everywhere else (but with nodes at RF cavities) by closed electric bumps.

ELECTRIC BUMP BUNCH SEPARATION

Operating Energies

Typical energies for "Higgs Factory" operation are established by the cross sections shown in Figure 1. We arbitrarily choose 120 GeV per beam as the Higgs particle operating point and identify the single beam energy this way in subsequent tables. Similarly identified are the Z_0 energy (45.6 GeV), the W-pair energy of 80 GeV, the LEP energy (arbitrarily taken to be 100 GeV) and the $t\bar{t}$ energy of 175 GeV to represent high energy performance.

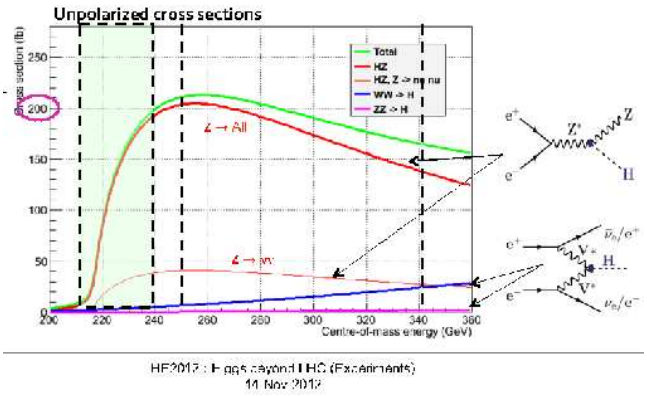

Figure 1: Higgs particle cross sections up to $\sqrt{s} = 0.3$ TeV (copied from Patrick Janot); $\mathcal{L} \geq 2 \times 10^{34}/\mathrm{cm}^2/\mathrm{s}$, will produce 400 Higgs per day in this range.

Bunch Separation at LEP

Much of the material in this section has been drawn from John Jowett's article "Beam Dynamics at LEP" [1]. When LEP was first commissioned for four bunches (N_b=4) and four IPs (N^*=4) operation, bunch collisions at the 45 degree points were avoided by vertical electric separation bumps. It was later realized that vertical bumps are inadvisable because of their undesirable effect on vertical emittance ϵ_y, which needs to be minimized. We therefore consider only horizontal separation schemes.

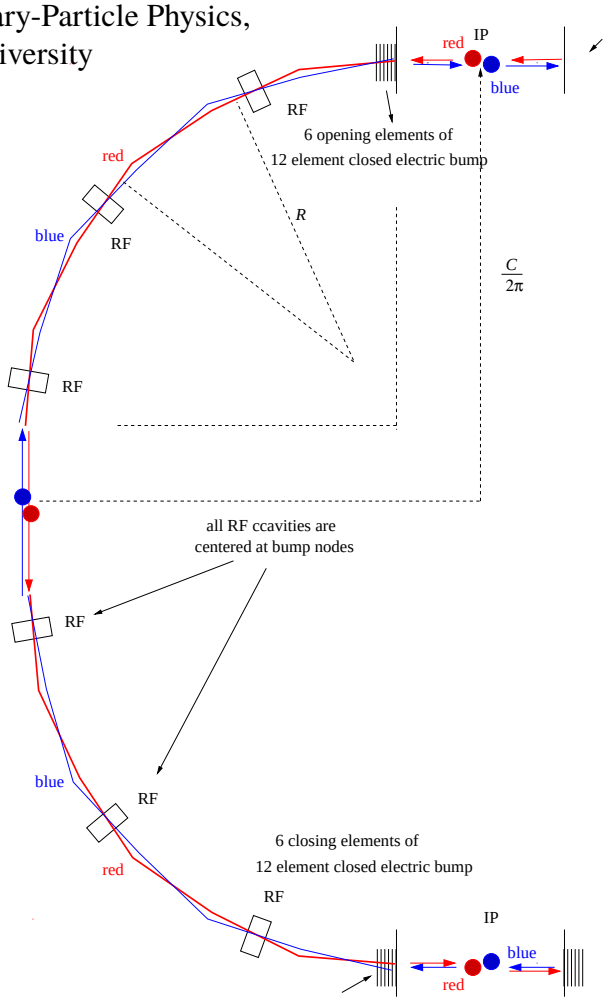

Figure 2: Cartoon illustrating beam separation in one arc of a Higgs factory. There are N_b=4 bunches in each beam and N^*=2 interaction points (IP). The bend radius R is significantly less than the average radius $C/(2\pi)$; roughly $C = 3\pi R$. For scaling purposes R and C are taken to be strictly proportional. Far more separation loops and crossovers are actually needed than are shown.

Various horizontal pretzel separation schemes were tried at LEP. They were constrained by the need to be superimposed on an existing lattice. LEP investigations in the early 1990's mainly concentrated on what now would be called quite low energies, especially the Z_0 energy, $E = 45.6$ GeV. For a Higgs factory we need to plan for energies four or five times higher. The required product of separator length multiplied by electric separator field has to be greater by the same factor to obtain the same angular separation. Actually the factor may have to be somewhat greater than this because of the larger bunch separation needed with increased ring circumference.

Before continuing, allow me a brief digression concerning the etymology of the technical and metaphorical term "pretzel". The term was coined by Raphael Littauer, the inventor of the eventually workable pretzel beam separation scheme. The pretzel "idea" first came to Boyce "Mac" McDaniel, director of the Cornell Laboratory of Nuclear Studies at the time.

As first realized by McDaniel, instead of having closed bumps one can make do with a single separator. The effect of a single electric deflection is to make the closed orbits of the counter-circulating beams different *everywhere*. Even in this case there are periodic "nodes" at which the distorted orbits cross. To achieve the desired beam separation, one has only to arrange for the desired crossing points to be at nodes and the parasitic crossing points to be at "loops" of the respective closed orbits. Raphael Littauer introduced the picturesque term "pretzel" to distill the entire discussion of this paragraph into a single word.

The original pretzel conception was not good enough, however, since the crossing angle at the IP was damaging to the luminosity. It was Littauer who fleshed out the idea and led its successful implementation. It proved necessary to introduce four electric separators in matched pairs about the North and South IP's. This invalidated the original name "pretzel" since the scheme amounted to closed electric bump separation separately in the East and West arcs. Nevertheless, by that time the name had caught on and the scheme continued to be called pretzel separation in CESR and in all subsequent rings.

A disadvantage of the metaphorical terminology is that it conveys a picture of the whole ring being a single "pretzel", obscuring the fact that the separation bumps are closed in each arc—two closed pretzels, if one prefers. To emphasize this point, for this paper only, I discuss closing electric multibumps, arc-by-arc. But what is being described is a pretzel separation scheme.

Separating the beam in a pre-existing ring is significantly more difficult than designing beam separation during the planning stage, as was done, for example, for the 45 degree separation points in the initial LEP ring. Obviously the separators have to be electric and therefore probably quite long. At CESR there was no free space long enough, so existing magnets had to be made shorter and stronger to free up space for electric separators. Even so, the required electric field was uncomfortably large.

With N_b equally-spaced bunches in each of the counter-rotating beams the beams need to be separated at the $2N_b - N^*$ "parasitic" crossing points. Standard closed bumps are typically π-bumps or 2π bumps. But, with 4 deflectors, two at each end of a sector, bumps can easily be designed to be $n\pi$ bumps, where n is an arbitrary integer matched to the desired number of separation points.

This discussion is illustrated pictorially in Figure 3 using a space-time plot introduced (in this context) by John Jowett. The beams are plotted as "world trajectories", whose crossings in space do not, in general, coincide with their crossings in time. Separated points with the same label correspond to the same point at different times.

In the figure, associating point 4 with point 1 would correspond to the original McDaniel pretzel scheme in which the counter-circulating orbits are different everywhere in the ring. With the "closed pretzels" there is no such association. The separated beams are smoothly merged onto common orbits at both ends.

(With care) one can associate the transverse bump displacement pattern with the space-time diagram, interpreting the vertical axis as bump amplitude. A head-on collision occurs when two populated bunches pass through the same space-time point. To avoid parasitic crossings the minimum bunch separation distance is therefore twice the closed bump period.

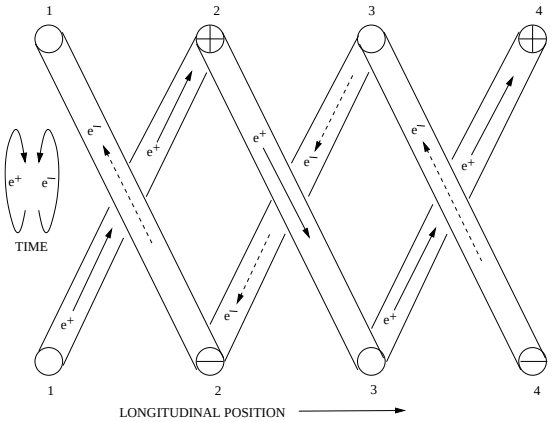

Figure 3: A minimal and modified "Jowett Toroidal Space-Time Beam Separation Plot" illustrating the separation of counter-circulating beams. Points with the same label at the top and the bottom of the plot are the same points (at different times). Though drawn to suggest a toroid the plot is purely two dimensional. The original McDaniel pretzel encompassed the whole ring—that is, in this figure, points 1 and 4 would also be identified. But this identification is not essential.

Another separation scheme tried at LEP was local electric bumps close to the 4 IP's and angle crossing to permit "trains" with more than one bunch per train. This permitted as many as 4 bunches per train though, in practice, more than 3 were never used. For lack of time this option is not considered in this paper.

The primary horizontal separation scheme at LEP is illustrated in Jowett's clear, but complicated, Figure 3 [1]. The scheme used 8 primary separators and 2 trim separators with the separation bumps continuing through the 4 IP's, but with vanishing crossing angles at all 4 IP's. Starting from scratch in a circular collider that is still on the drawing board, one hopes for a simpler separation scheme.

Separated Beams and RF Cavities

By introducing slightly shortened, slightly strengthened, special purpose bending magnets to make space for electric separators, multi-element electric bumps can be located

arbitrarily without seriously perturbing any existing lattice design. But there is an issue with separated orbits and RF cavities. Probably both beams should pass through the centers of the RF cavities. But it seems safe to assume that the closed orbit angles through the RF can be (symmetrically) different from zero. Otherwise, far more electric separators will be required, and far fewer bunches would be possible. RF cavities are therefore to be placed at beam separation nodes. (This may complicate betatron tune tunability?)

"Topping-off" injection is essential; especially to permit large beam-beam tune shifts. As long as the beam current is constant the beam-beam deflection is equivalent to an ideal lens, focusing in both planes, though with strong octupole superimposed. The linear focusing part can be incorporated into the (linear) lattice optics. And the superimposed octupole is not necessarily very damaging. Strong damping makes bump-free, kicker-free, bunch-by-bunch, high-efficiency, vertical injection possible. Then steady-state, continuous operation without fill cycling may be possible.

Somewhat reduced beam separation at bump ends is assumed to be acceptable. With crossing angle the number of bunches may later be increased.

6 + 6 ELEMENT CLOSED ELECTRIC BUMP

Bunches must not collide in arcs. They should be separated by at least 10 beam width sigmas when they pass. With both beams passing through the same RF, the path lengths between RF cavities probably have to be equal. A single ring is as good as dual rings if the total number of bunches can be limited to, say, less than 200. Here it is proposed to support only head-on collisions at each of the two IP's. The minimum bunch spacing will then be slightly greater than the total length of the intersection region (IR).

The half ring shown in Figure 2 shows a closed electric bump in the west arc. Orbits are common only in the two IR's. On the exit from each IR an electric bump is started and the bump is closed just before the next IR. These "bumps" are very long, almost half the circumference. As already explained, this is not "pretzel" beam separation, as that term was initially understood. Other than being horizontal rather than vertical and having multiple avoided parasitic collisions, these are much like the four separation bumps in the original LEP design.

Closed bumps require at least 3, or for symmetry, 4 controllable deflectors. Here a 12-bump scheme is described, with 6 electrostatic separators at the bump start and 6 at the bump stop. This scheme could be needed if the lattice cell lengths are too short to contain sufficiently strong electric separators. In my WG6 paper I show that the optimal collider cell length L_i is significantly longer than was assumed when this separation scheme was designed. With longer cells a simpler 4 or 6 kicker bump may be adequate.

The design orbit spirals in significantly; this requires the RF acceleration to be distributed quite uniformly. Basically the ring is a "curved linac". The only betatron tune tunability is in the arcs. As the arc phase advances are changed (by a percent or so) the bumps have to be closed (very accurately) by tuning phase advance per cell and electric separators. As with beam separation in LEP, trim separators may be required.

Sketches and design formulas for a multi-element electric bump are shown in Figure 4. Figure 5 exhibits the separation of up to 112 bunches in a 50 km ring. Notice that, to avoid head-on parasitic collisions, the bunch separations are equal to two wavelengths of the electric bump pattern.

BUNCH SEPARATION PARTITION NUMBER SHIFT

(Mangling Jowett's careful formulation [1] for brevity) the longitudinal partition number J_ϵ depends on focusing function K_1, dispersion D, and on fractional momentum offset, $\delta = \bar{\delta} + \delta_{s.o.}$ (where "s.o." stands for synchrotron oscillation) and separator displacement $x_p(s)$;

$$J_\epsilon(\delta, x_p) = 2 + \frac{2\oint K_1^2 D^2 ds}{\oint (1/R^2) ds}\,(\bar{\delta} + \delta_{s.o.}) + \\ + \frac{2\oint K_1^2 (D(s) - D_0(s)) x_p(s) ds}{\oint (1/R^2) ds}; \quad (1)$$

here D/D_0 are the separator-on/separator-off horizontal dispersion functions. The middle term here can be used to shift J_ϵ away from 2, as proved useful at LEP, but it does not depend on x_p; it is shown only as protection against confusing it with the final term.

Setting $\bar{\delta} + \delta_{s.o.}$=0, and averaging, the separator-displaced partition number is

$$J_\epsilon(|x_p|) = 2 + \frac{2 < K_1^2 (D - D_0) x_p >}{< 1/R^2 >}. \quad (2)$$

In spite of x_p averaging to zero, there is a non-vanishing shift of $J_\epsilon(|x_p|)$ because K_1, D, and x_p are correlated. At LEP this shift was observed to be significanly damaging and to be dominated by sextupoles. The factors in Eq. (2) scale as

$$x_p \propto \sigma_x \propto \frac{1}{R^{1/2}}, \quad K_1 = \frac{q}{l_q} \propto \frac{1/R^{1/2}}{R^{1/2}} \propto \frac{1}{R}, \\ D - D_0 \propto S \propto \frac{1}{R^{1/2}}, \quad \Delta J_\epsilon(|x_p|) \propto \frac{1}{R}. \quad (3)$$

These scaling formulas (derived in my WG 6 report) indicate that the seriousness of this partition number shift actually decreases with increasing R. Even if this were not true, should the partition number shift be unacceptably large, it can be reduced by increasing the quadrupole length l_q to decrease K_1. The partition number shift is due to excess radiation in the quadrupoles. Since this radiation intensity is proportional to the square of the magnetic field, doubling the quadrupole length halves the radiation and the partition number shift.

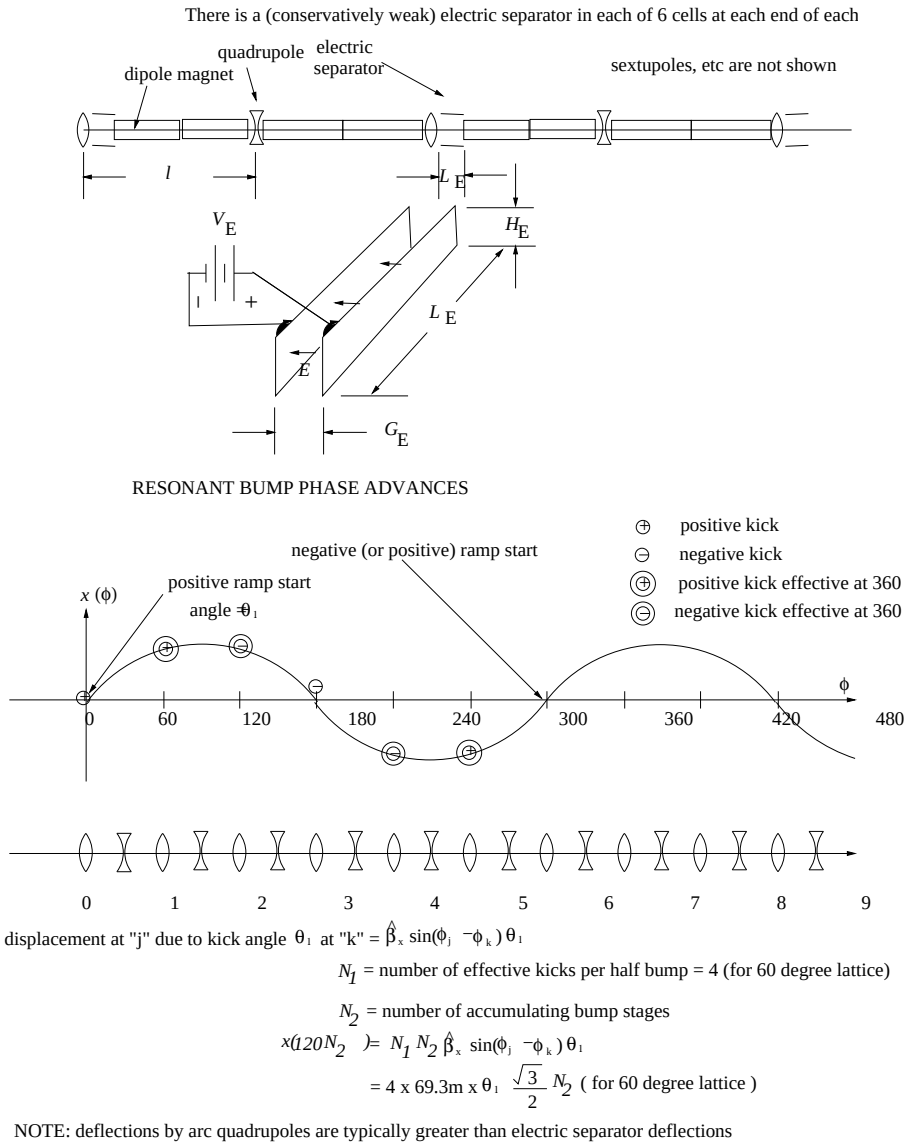

Figure 4: Sketches and design formulas for a multi-element electric bump.

BEAM SEPARATION IN INJECTION-OPTIMIZED COLLIDER LATTICE

The beam separation scheme shown so far has used a very short collider cell length $L_c = 60\,\mathrm{m}$. Table 1 (which is explained in my W6 paper) describes the scaling of lattice parameters obtained after redesigning both injector and collider for efficient injection. The resulting collider cell length is $L_c = 213\,\mathrm{m}$. Because the cells are so long, there may be no need for multiple electrostatic separators. Instead one may use, for example, two or three electric kickers to launch each electric bump, with two or three matched kickers to terminate it. A large increase in cell length will surely also require a corresponding increase in longitudinal separation of circulating bunches. The single beam luminosity will be correspondingly reduced if the luminosity is already limited by the maximum number of bunches, as in the case of Z_0 production. The luminosity reduction should be little affected at the Higgs energy and above.

Irrespective of bunch separation schemes, the minimum bunch separation will still be at least equal to the length of the intersection region. For single ring operation this will probably be less restrictive than the bunch separation required for the separation scheme.

PREDICTED LUMINOSITIES

With one 100 km circumference ring, the maximum number of bunches is limited to about 200. For $N_b < 200$ the luminosity $\mathcal{L}$ has to be reduced proportionally. $\mathcal{L} \rightarrow \mathcal{L}_{\mathrm{actual}} = \mathcal{L} \times N_b/200$. Luminosities in the $100\,km$, 25 MW case are given in my WG2 report "Ring Circumference and Two Rinfs vs One Ring". Here, for comparison, and to more

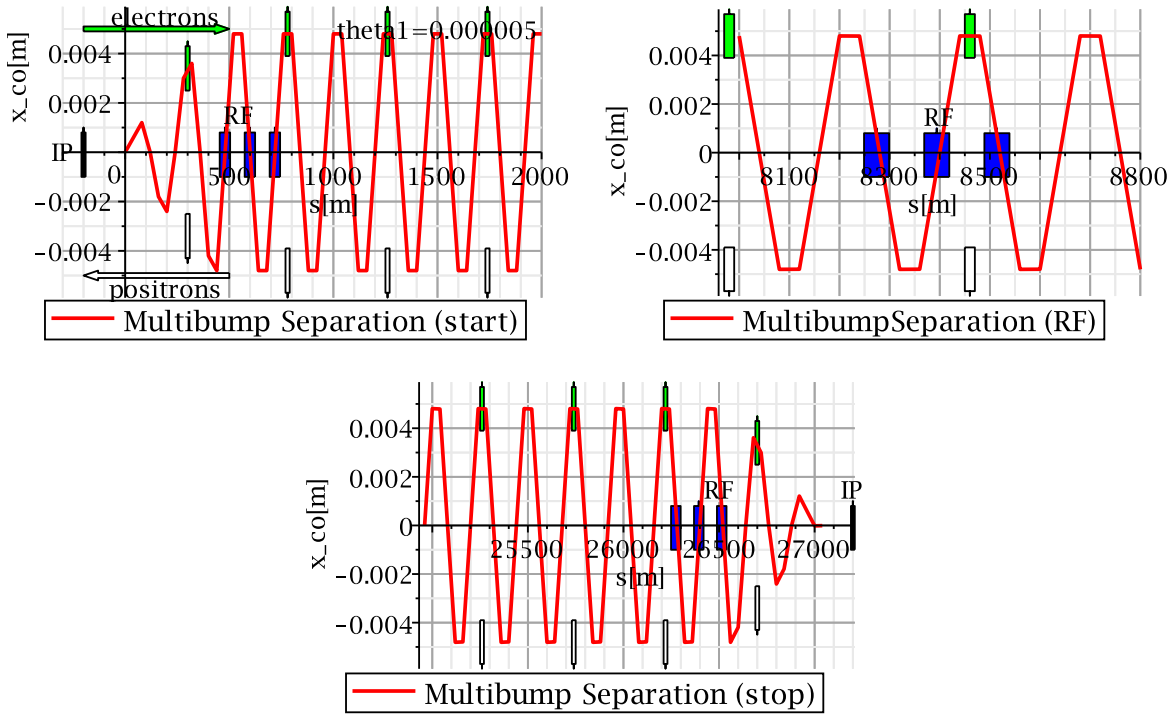

Figure 5: Short partial sections of the multibump beam separation are shown: one at the beginning, one at an RF location in the interior, and one at the far end of a long arc in Figure 2. The bunch separations are 480 m in a 50 km ring with cell length L_c = 60 m. IP's are indicated by vertical black bars, RF cavities by blue rectangles, electron bunches are green rectangles moving left to right, positron bunches are open rectangles moving from right to left. Counter-circulating bunches are separated at closed bump loop locations, and they must not pass through the nodes at the same time.

nearly match the separation scheme shown in Figure 5, the circumference is assumed to be C=50 km, the RF power 50 MW per beam, and the number of bunches N_b=112. The results are shown in Table 3 (unlimited N_b) and Table 4 (with N_b=112).

The values of parameters not shown in the tables are η_{Telnov}=0.01, β_y^* =5 mm, $xi^{\text{typ.}}/\beta_y^*$=22.8, τ_{bs}=600 s, Optimistic= 1.5, $R_{\text{Gau-unif}}$=0.30, eV_{rf}=20 GeV, $OV_{\text{req.}}$=20 GV, a_{xy}=15, r_{yz}=1, $\beta_{x,\text{arcmax}}$=120 m.

REFERENCES

[1] J. Jowett, *Beam Dynamics at LEP,*CERN SL/98-029 (AP), 1998

[2] J. Jowett, *More Bunches with Pretzel,* Private communication "pzl6.dvi".

[3] R. Talman, *Specific Luminosity Limit of e+/e- Colliding Rings,*Phys. Rev. ST-AB, 2002

Parameter	Symbol	Proportionality	$L \propto R^{3/4}$ collider	Values C=100 km
phase advance per cell	μ_x		90°	
cell length	L		$R^{3/4}$	213 m
bend angle per cell	ϕ	$= L/R$	$R^{-1/4}$	
quad strength $(1/f)$	q	$1/L$	$R^{-3/4}$	
dispersion	D	ϕL	$R^{1/2}$	
beta	β	L	$R^{3/4}$	
tune	Q_x	R/β	$R^{1/4}$	125.26
tune	Q_y	R/β	$R^{1/4}$	105.19
Sands's "curly H"	$\mathcal{H}$	$= D^2/\beta$	$R^{1/4}$	
partition numbers	$J_x/J_y/J_\epsilon$	1/1/2	1/1/2	
horizontal emittance	ϵ_x	$\mathcal{H}/(J_x R)$	$R^{-3/4}$	
fractional energy spread	σ_δ	$\sqrt{B}$	$R^{-1/2}$	
arc beam width-betatron	$\sigma_{x,\beta}$	$= \sqrt{\beta\epsilon_x}$	1	
-synchrotron	$\sigma_{x,synch.}$	$= D\sigma_\delta$	1	
sextupole strength	S	q/D	$R^{-5/4}$	
dynamic aperture	$x^{\max}$	q/S	$R^{1/2}$	
relative dyn. aperture	$x^{\max}/\sigma_x$		$R^{1/2}$	
separator amplitude	x_p	σ_x	1	

Table 1: Scaling of collider lattice parameters for improved injection efficiency collider.

Parameter	Symbol	LEP-extrapolated	Unit	Collider	
mean bend radius	R	**3026**	m	**5675**	**11350**
beam energy		120	GeV	120	120
circumference	C	26.7	km	50	100
cell length	L	79	m	127	213
momentum compaction	α_c	1.85e-4	m	1.35e-4	0.96e-4
tunes	Q_x	90.26		105.26	125.26
	Q_y	76.19		89.19	105.19
partition numbers	$J_x/J_y/J_\epsilon$	1/1.6/1.4		1/1/2	1/1/2
main bend field	B_0	0.1316	T	0.0702	0.0351
energy loss per turn	U_0	6.49	GeV	3.46	1.73
radial damping time	τ_x	0.0033	s	0.0061	0.0124
	τ_x/T_0	37	turns	69	139
fractional energy spread	σ_δ	0.0025		0.0013	0.0009
emittances (no BB), x	ϵ_x	**21.1**	nm	**13.2**	**7.82**
y	ϵ_y	1.0	nm	0.66	0.39
max. arc beta functs	$\beta_x^{\max}$	125	m	200	337
max. arc dispersion	$D^{\max}$	0.5	m	0.68	0.97
quadrupole strength	$q \approx \pm 2.5/L_p$	0.0316	1/m	0.0197	0.0117
max. beam width (arc)	$\sigma_x = \sqrt{\beta_x^{\max}\epsilon_x}$	1.6	mm	1.625	1.558
(ref) sextupole strength	$S = q/D$	0.0632	$1/m^2$	0.0290	0.0121
(ref) dynamic aperture	$x^{\mathrm{da}} \sim q/S$	~0.5	m	~0.679	~0.967
(rel-ref) dyn.ap.	x^{da}/σ_x	~0.313		~0.417	~0.621
separator amplitude	$\pm 5\sigma_x$	±8.0	mm	±8.1	±7.8

Table 2: Parameters values scaled from LEP.

name	E	ϵ_x	β_y^*	ϵ_y	ξ_{sat}	N_{tot}	σ_y	σ_x	u_c^*	$n_{\gamma,1}^*$	$\mathcal{L}^{\text{RF}}$	$\mathcal{L}_{\text{trans}}^{\text{bs}}$	$\mathcal{L}^{\text{bb}}$	N_b	β_x^*	P_{rf}
	GeV	nm	mm	pm			μm	μm	GeV		10^{34}	10^{34}	10^{34}		m	MW
Z	46	0.916	2	61.1	0.094	7.3e+14	0.35	5.24	0.000	1.97	52.5	96.8	52.513	33795	0.03	50
W	80	0.323	2	21.6	0.101	7.6e+13	0.208	3.12	0.001	2.06	9.66	16.2	9.661	5696	0.03	50
LEP	100	0.215	2	14.3	0.101	3.1e+13	0.169	2.54	0.002	2.10	4.95	8	4.947	2814	0.03	50
H	120	0.153	2	10.2	0.102	1.5e+13	0.143	2.15	0.003	2.13	2.86	4.48	2.863	1581	0.03	50
tt	175	0.077	2	5.12	0.118	3.3e+12	0.101	1.52	0.006	2.19	0.923	1.35	0.923	478	0.03	50
Z	46	16.5	5	1100	0.094	7.3e+14	2.35	35.21	0.001	2.12	21	33.2	21.005	1872	0.075	50
W	80	5.88	5	392	0.101	7.6e+13	1.4	20.99	0.003	2.22	3.86	5.52	3.864	313	0.075	50
LEP	100	3.91	5	261	0.101	3.1e+13	1.14	17.12	0.005	2.26	1.98	2.71	1.979	154	0.075	50
H	120	2.80	5	187	0.102	1.5e+13	0.966	14.50	0.007	2.30	1.15	1.52	1.145	86	0.075	50
tt	175	1.41	5	94	0.118	3.3e+12	0.686	10.28	0.016	2.38	0.369	0.455	0.369	26	0.075	50
Z	46	149	10	9900	0.094	7.3e+14	9.95	149.28	0.002	2.24	10.5	14.7	10.503	208	0.15	50
W	80	53.1	10	3540	0.101	7.6e+13	5.95	89.26	0.007	2.36	1.93	2.42	1.932	34	0.15	50
LEP	100	35.4	10	2360	0.101	3.1e+13	4.86	72.88	0.011	2.41	0.989	1.19	0.989	17	0.15	50
H	120	25.4	10	1700	0.102	1.5e+13	4.12	61.78	0.016	2.45	0.573	0.663	0.573	9.5	0.15	50
tt	175	12.9	10	857	0.118	3.3e+12	2.93	43.92	0.035	2.54	0.185	0.198	0.185	2.9	0.15	50

Table 3: Luminosity influencing parameters and luminosities with unlimited number of bunches N_b, assuming 50 km circumference ring and 50 MW per beam RF power.

E	β_y^*	ξ_{sat}	$\mathcal{L}_{\text{actual}}$	N_{actual}	P_{rf}
GeV	m		10^{34}		MW
46	0.002	0.094	0.174	112	50
80	0.002	0.1	0.190	112	50
100	0.002	0.1	0.197	112	50
120	0.002	0.1	0.203	112	50
175	0.002	0.12	0.216	112	50
46	0.005	0.094	1.256	112	50
80	0.005	0.1	1.380	112	50
100	0.005	0.1	1.434	112	50
120	0.005	0.1	1.145	86.6	50
175	0.005	0.12	0.369	26.1	50
46	0.010	0.094	5.644	112.0	50
80	0.010	0.1	1.932	34.7	50
100	0.010	0.1	0.989	17.1	50
120	0.010	0.1	0.573	9.5	50
175	0.010	0.12	0.185	2.9	50

Table 4: Luminosity influencing parameters and luminosities with the number of bunches limited to $N_b = 112$, assuming 50 km circumference ring and 50 MW per beam RF power.